Neurobiology of Stress 15 (2021) 100390

Contents lists available at ScienceDirect

Neurobiology of Stress

journal homepage: www.elsevier.com/locate/ynstr

Erasing m^{6}A-dependent transcription signature of stress-sensitive genes triggers antidepressant actions

Peng-Fei Wu [a,b,c,d,e,1], Qian-Qian Han [a,b,1], Fu-Feng Chen [a,b], Tian-Tian Shen [a,b], Yi-Heng Li [a,b], Yu Cao [a,b], Jian-Guo Chen [a,b,c,d,e], Fang Wang [a,b,c,d,e,*]

[a] Department of Pharmacology, School of Basic Medicine, Tongji Medical College, Huazhong University of Science and Technology, Wuhan City, Hubei, 430030, China
[b] The Research Center for Depression, Tongji Medical College, Huazhong University of Science, 430030, Wuhan, China
[c] Key Laboratory of Neurological Diseases (HUST), Ministry of Education of China, Wuhan City, Hubei, 430030, China
[d] The Key Laboratory for Drug Target Researches and Pharmacodynamic Evaluation of Hubei Province, Wuhan City, Hubei, 430030, China
[e] Laboratory of Neuropsychiatric Diseases, The Institute of Brain Research, Huazhong University of Science and Technology, Wuhan, 430030, China

ARTICLE INFO

Keywords:
Depression
Stress vulnerability
Tricyclic antidepressant
N^6-methyladenosine
FTO

ABSTRACT

Emerging evidence has shown that stress responsivity and psychiatric diseases are associated with alterations in N^6-methyladenosine (m^{6}A) mRNA epigenetic modifications. Fat mass and obesity-associated protein (FTO) is an m^{6}A demethylase that has been linked to increased body mass and obesity. Here, we show that tricyclic antidepressants (TCAs) with weight-gain side effects, such as imipramine and amitriptyline, directly increased FTO expression and activated its epigenetic function in the ventral tegmental area (VTA). VTA-specific genetic disruption of FTO increased stress vulnerability and abolished the antidepressant activity of TCAs, whereas erasing m^{6}A modification in the VTA by FTO overexpression or cycloleucine led to significant antidepressant activity. Mechanistically, both transcriptome sequencing and quantitative PCR revealed that overexpression of FTO in the VTA decreased the transcription of stress-related neuropeptides, such as cocaine- and amphetamine-regulated transcript peptide and urocortin, in the social defeat model, which was mimicked by imipramine, suggesting an m^{6}A-dependent transcription mechanism of stress-related neuropeptides may underlie the responses to antidepressant. Collectively, our results demonstrate that inhibiting m^{6}A-dependent transcription of stress-related genes may work as a novel antidepressant strategy and highlight a previously unrecognized activator of FTO-dependent epigenetic function that may be used for the treatment of other neurological diseases.

1. Introduction

N^6-methyladenosine (m^{6}A), the most abundant and conserved internal transcript modification on eukaryotic messenger RNA (mRNA) molecules, plays important roles in various neurobiological processes (Chen et al., 2019; Edens et al., 2019; Merkurjev et al., 2018; Widagdo et al., 2016; Wu et al., 2019), such as learning and memory, synaptic transmission, neurogenesis and neural differentiation, by regulating mRNA transcript processing and translation. The formation of m^{6}A is catalyzed by a methyltransferase complex (Methyltransferase-like 3, METTL3; methyltransferase-like 14, METTL14 and Wilms tumor 1-associated protein, WTAP) and erased by demethylases, including fat mass- and obesity-associated (FTO) protein and the α-ketoglutarate-dependent dioxygenase alkB homolog 5 (ALKBH5) protein (Jia et al., 2011; Liu et al., 2014; Ping et al., 2014; Wang et al., 2016; Zheng et al., 2013). Emerging evidence indicates that aberrant m^{6}A may be considered a new layer of epigenetic mechanisms underlying the pathogenesis of psychiatric diseases, such as cocaine addiction (Hess et al., 2013), alcohol use disorder (Bohnsack et al., 2019) and Alzheimer's disease (Shafik et al., 2021). For major depressive disorder (MDD), a recent study demonstrated that the location and time of stress exposure alter m^{6}A modifications (Engel et al., 2018). Another recent report revealed that m^{6}A methylation of fatty acid amide hydrolase messenger RNA in the hippocampus (Hip) may be involved in the regulation of MDD (Huang et al., 2020). However, precisely how m^{6}A methylation in different brain regions is involved in MDD is far from clear.

* Corresponding author.Department of Pharmacology, School of Basic Medicine, Tongji Medical College, Huazhong University of Science and Technology, Wuhan City, Hubei, 430030, China.
E-mail address: wangfanghust@mail.hust.edu.cn (F. Wang).
[1] These authors contributed equally in the study.

https://doi.org/10.1016/j.ynstr.2021.100390
Received 4 June 2021; Received in revised form 8 August 2021; Accepted 3 September 2021
Available online 4 September 2021

The discovery of FTO as the first m^6A eraser establishes the concept of reversible RNA modification. FTO knockout mice exhibit neuropsychiatric phenotypes that include anxiety-like behaviors (Spychala and Ruther, 2019), memory deficits (Li et al., 2017a; Spychala and Ruther, 2019), abnormal fear coping (Engel et al., 2018), decreased brain size (Li et al., 2017a), reduced body weight (Li et al., 2017a), and impaired neurogenesis (Gao et al., 2020; Li et al., 2017a) and neurotrophic signaling (Spychala and Ruther, 2019). These lines of evidence point to a possible antidepressant role of FTO. Although some pharmacological inhibitors of FTO have been identified, including rhein (Chen et al., 2012), R-2-hydroxyglutarate (Su et al., 2018) and entacapone (Peng et al., 2019), very little is known about pharmacological activators of FTO. Before its role as a demethylase was confirmed, FTO originally attracted attention as an obesity- and diabetes-related protein due to the link between its genetic polymorphism and the body mass index of humans (Frayling et al., 2007). Interestingly, FTO overexpression leads to increased food intake (Church et al., 2010), which are often observed as side effects in patients taking antipsychotic medicines, such as tricyclic antidepressants (TCAs) (Berken et al., 1984; Salvi et al., 2018). Given the predicted association of FTO with antipsychotic-induced weight gain (Shing et al., 2014) and MDD-related brain functions, exploring its role in TCAs pharmacology is a promising research pursuit.

As the first class of antidepressants has been used clinically for over half a century, the real pharmacological mechanisms of TCAs are not fully understood. The previously held hypothesis that TCAs act by inhibiting monoamine uptake has been questioned because their rapid effect on monoamines contrasts with delayed antidepressant effects. The rise of several other theories in TCA pharmacology, including the neurogenesis hypothesis, the acid sphingomyelinase-ceramide hypothesis and the autophagy hypothesis, profoundly inspired research on the pathophysiological mechanism of MDD (Gulbins et al., 2013, 2018; Kornhuber et al., 2014; Santarelli et al., 2003). Here, we identified TCAs as previously unrecognized activators of FTO-dependent epigenetic function and highlighted FTO as a primary antidepressant target that reverses stress-induced transcriptome changes.

2. Material and methods

2.1. Animals and behavioral experiments

Adult male C57BL/6J mice (6–8 weeks old) were purchased from Hunan SJA Laboratory Animal (Changsha, Hunan, China). Male CD-1 retired breeder mice ranging from 8 to 10 months old were obtained from Vital River Laboratory Animal Technology Co. Ltd (Beijing, China) and individually housed. Animals were maintained under standard laboratory conditions with a 12-h light/dark cycle at a constant temperature (22 ± 2 °C) and humidity (40%–60%), and provided ad libitum access to food and water. All procedures were conducted following the Declaration of Helsinki and the Guide for Care and Use of Laboratory Animals as adopted and promulgated by the National Institutes of Health and approved by the Review Committee for the Use of Human or Animal Subjects of the Huazhong University of Science and Technology. The mice from all experimental groups were imaged in a random order. The required sample size was estimated based on prior experiments to satisfy the 3Rs (replacement, reduction, and refinement) principle of ethical use of experimental animals.

The procedure of chronic social defeat stress (CSDS) was performed as we previously reported (He et al., 2021; Li et al., 2018). Briefly, aggressive CD-1 mice were used as residents to defeat C57BL/6J mice (intruders) for 5–10 min per day over 10 consecutive days. C57BL/6J mouse were then housed with CD-1 mouse in a cage divided by a transparent clipboard. The shared home cage allowed sensory (visual, olfactory, auditory) contact between the C57BL/6J mouse and CD-1 mouse to enable continuous sensory defeat. After the 10 day, C57BL/6J mouse was returned to a single cage overnight and carry out social interaction testing (SIT) and a sucrose preference test (SPT) on the following day. For subthreshold social defeat stress (SSDS) (Li et al., 2017b), mice were exposed to three social defeat sessions: 5 min defeat bouts followed by a 15 min inter trial interval between the defeats.

SIT and SPT were performed to evaluate the depressive-like behavior after CSDS according to previous studies from our group and other labs (Friedman et al., 2016; He et al., 2021; Li et al., 2018; Yohn et al., 2019). After CSDS treatment, animals were subjected to SIT and SPT to identify the susceptible mice. Only the mice with both interaction ratio <1.0 in SIT and sucrose preference <75% in SPT were considered susceptible, and 14 days of vehicle or drug injection was indistinctly administered to susceptible mice. Immobility time in tail suspension test (TST) and forced swim test (FST) of normal animals are widely used models in antidepressants screening, and a previous study has indicated that social defeat stress exerted little effects on the TST and FST (Klinsey et al., 2007). Thus, TST, FST, open field test (OFT) and elevated plus maze (EPM) were performed in normal mice as we previously reported (He et al., 2021; Li et al., 2018). Detailed methods for behavioral experiments were available in *Supplemental Information*.

2.2. Cell culture and drug treatments

Mouse neuroblastoma 2A (N2a) cell line was obtained from the China Biological Part Stock Center (Beijing, China) and cryopreserved after subculturing different passages. N2a cells were routinely propagated using Dulbecco's Modified Eagle Medium (DMSO, Gibco Laboratories, Grand Island, NY, USA), supplemented with 10% fetal bovine serum (Gibco Laboratories, Grand Island, NY, USA) and 100 U/mL penicillin and 100 μg/mL streptomycin (Gibco Laboratories, Grand Island, NY, USA) in a humidified incubator of 5% CO_2 at 37 °C. Cultured cells were incubated for 48 h with pharmacological agents at the following concentrations: 0.1% DMSO (vehicle), 10 μM imipramine (IMI; Sigma-Aldrich, St. Louis, MO, USA), 10 μM amitriptyline (AMT; Aladdin, Shanghai, China), 10 μM mirtazapine (TCI, Tokyo, Japan), 10 μM fluoxetine (Sigma-Aldrich, St. Louis, MO, USA). Then, RNA was extracted from the N2a cells with Trizol (Takara Bio, Tokyo, Japan).

2.3. Tissue collection

Coronal brain slices (300 μm) containing the ventral tegmental area (VTA), medial prefrontal cortex (mPFC), Hip and nucleus accumbens (NAc) were cut by a vibratome (Leica, Wetzlar, Germany) in ice-cold artificial cerebrospinal fluid (ACSF) containing 119 mM NaCl, 1.3 mM $MgSO_4$, 3.5 mM KCl, 11.0 mM glucose, 26.2 mM $NaHCO_3$, 1.0 mM NaH_2PO_4 and 2.5 mM $CaCl_2$, pH 7.4, which was oxygenated with 95% O_2 + 5% CO_2. The certain brain subregions, including the mPFC, Hip and VTA, were dissected thoroughly under the dissecting microscope using a special blade in accordance with the histology atlas of Paxinos and Franklin (2001, The Mouse Brain in Stereotaxic Coordinates 2nd edn, San Diego, CA: Academic) to perform molecular experiments.

2.4. Stereotaxic surgery

After CSDS exposure, mice were subjected to SIT and SPT before the cannulation to identify the susceptible group, and only the mice with both interaction ratio <1.0 in SIT and sucrose preference <75% in SPT were considered susceptible and performed cannulation. Susceptible or control mice were anesthetized with an intraperitoneal injection (i.p.) of pentobarbital sodium (45 mg/kg; Sinopharm, Shanghai, China). Subsequently, mice were placed in a small-animal stereotaxic device, which was washed with swabs containing 75% ethanol. Surgical tools were sterilized with 75% ethanol. The skull was exposed and gently thinned using a dental drill around the VTA region. Twenty-two-gauge stainless steel guide cannulas (RWD, Shenzhen, China) were bilaterally implanted in the VTA region (AP = −3.3 mm, ML = 0.5 mm, DV = − 4.4 mm). The mice were allowed to recover for 1 week after surgery. Cycloleucine (40 μg/μL/side, Sinopharm, Shanghai, China), betaine (20 μg/μL/side,

Sinopharm, Shanghai, China), rhein (1 μg/μL/side, Aladdin, Shanghai, China), recombinant urocortin (1 μg/μL/side, Cloud-Clone Crop, Wuhan, China) and recombinant cocaine and amphetamine regulated transcript (CART, 0.5 μg/μL/side, Immuno Clone Biosciences Co., Ltd, Huston, USA) were microinjected into the VTA through the cannulas with the microsyringe pump. Saline was used as the vehicle for IMI, AMT, mirtazapine and fluoxetine. The ACSF was used as the vehicle for cycloleucine, betaine, recombinant urocortin and recombinant CART. The ACSF containing 1‰ DMSO was used as the vehicle for rhein.

2.5. Genetic approaches

The third generation of self-inactivating lentivirus vector, which contains a CMV-driven enhanced green fluorescent protein (GFP) reporter and a U6 promoter upstream of cloning restriction sites (*Hpa*I and *Xho*I) to allow the introduction of oligonucleotides encoding short hairpin RNAs (shRNAs), was purchased from Shanghai Genechem Co., Ltd. The targeted sequence of *FTO* (referred as "LV-sh*FTO*") was 5′-ATACAAACTTTGCACCGAT-3′, and for control scrambled shRNA (referred as "LV-shCON") was 5′-TTCTCCGAACGTGTCACGT-3'. For *in vivo* lentiviral microinjections, lentiviral vector (2 μL) was bilaterally targeted to the VTA region at a rate of 0.1 μL/min followed by a 10 min rest period to prevent backflow. Mice were allowed to recover for 2–3 weeks before experiments.

For FTO overexpression, AAV-CMV-βGlobin-FTO-3Flag-SV40Poly A (referred as "AAV-FTO") or AAV-CMV-βGlobin-MCS-EGFP-MCS- 3Flag-Poly A (referred as "AAV-GFP") was purchased from Shanghai Genechem Co., Ltd. AAV-FTO (0.3 μL) was infused into the VTA at a rate of 0.05 μL/min followed by a 10 min rest period to prevent backflow. After 4 weeks, mice were sacrificed and GFP fluorescence in target brain regions were estimated to confirm the viral infection.

2.6. Immunofluorescence staining

To measure m^{6}A level by immunofluorescent staining, N2a cells were seeded onto coverslips in a 24-well plate and administrated with IMI or AMT for 48 h. Then cells were washed in phosphate buffer saline, fixed using 4% paraformaldehyde for 15 min at room temperature and treated with 3% bovine serum albumin (BSA) and 0.1% Triton X-100 in phosphate buffer saline for 30 min. The coverslips were incubated with mouse anti-m^{6}A antibody (202111, Synaptic Systems, Gottingen, Germany) at 1:250 dilution in 1% BSA overnight at 4 °C. Alexa-Fluor 594 (red, 1:1000; A21203, Invitrogen, California, USA) tagged anti-mouse monoclonal secondary antibody at 1:1000 dilution in 1% BSA was added for all fluorescent labeling. Images were acquired with a laser scanning microscope (FV1000, Olympus, Tokyo, Japan). A semi-quantitative analysis was conducted based on different staining intensities using Image J software. Images from confocal microscopes were acquired in a 16-bit setting. The level of m^{6}A was calculated as staining intensity/staining area. Results were expressed as a relative intensity ratio and normalized to the control group.

2.7. m^{6}A dot blot

The m^{6}A dot blot assay was performed as previously described with some modifications (Li et al., 2017b). Briefly, the indicated amount of total RNA (400 ng, 200 ng, 100 ng and 50 ng) was denatured in 1-fold volume of RNA incubation buffer (22.5% formaldehyde solution in 10 × Saline Sodium Citrate buffer) 50 °C for 20 min. And then RNA samples were applied to nitrocellulose membrane (BS-NC-22, Biosharp, Hefei, China) with a Bio-Dot Apparatus (BioRad, California, USA). After UV crosslinking, membrane was stained with 0.02% methylene blue in 0.3 M sodium acetate. After washing with 1 × TBST buffer for three times (10 min every time), membranes were blocked with 5% BSA in TBST for 1 h at room temperature. After that, blots were incubated with anti-m^{6}A antibody overnight at 4 °C. After rinsing in TBST, the blots were incubated for 1 h at room temperature with horseradish peroxidase-conjugated secondary antibodies (1:1000; Thermo Fisher Scientific, Massachusetts, USA). Finally, the immunoblot was completely immersed in enhanced chemiluminescence reagents (SuperSignal ECL kit; Thermo Fisher Scientific, Massachusetts, USA), and the blot reaction was revealed by MicroChemi (DNR Bio-Imaging Systems, Jerusalem, Israel).

2.8. Methylated RNA immunoprecipitation-quantitative PCR (meRIP-qPCR)

MeRIP assay was adjusted from reported protocol (Dominissini et al., 2013; Yue et al., 2015). Briefly, around 4–5 μg intact poly-A-purified RNA was fragmented into ~100-nt using RNA Fragmentation Reagents (AM8740, Invitrogen, California, USA) under 70 °C for 10 min followed by ethanol precipitation and collection. The m^{6}A-specific antibody was incubated with 60 μL dynabeads anti-mouse IgG (11033, Invitrogen, California, USA) in 0.5 mL immunoprecipitation buffer (10 mM sodium phosphate, 1M NaCl and 0.05% Triton-X) for overnight at 4 °C with rotation. Then the fragment mRNAs were incubated with antibody-beads mixture in 0.5 mL immunoprecipitation buffer for 4 h at 4 °C. Next, the mRNA-antibody-beads complex was eluted with elution buffer (5 mM Tris-HCL, pH 7.5, 1 mM EDTA, PH 8.0, 0.05% SDS, 20 mg/mL Proteinase K) at 50 °C for 1.5 h with vibrating. Then, supernatant was collected and precipitated with 1 μg glycogen, one-tenth volumes of 3 M sodium acetate in 2.5 vol of 100% ethanol at −80 °C overnight. Final mRNA sample was brought up in water and m^{6}A enrichment was detected by qPCR analysis. RNA from MeRIP was quantified by $2^{-\Delta\Delta ct}$ against non-immunoprecipitated input RNA. Primers used for MeRIP-qPCR are as follows: *Ucn*: 5′-CAAGGCGTCTTCAGCCCGT-3′, 5′-CATGGTGCCGCAGGTTATCG-3'; *Cartpt*: 5′-GCGCTATGTTGCAGATCGAA-3′, 5′-CAGTCACACAGCTTCCCGAT-3'.

2.9. Statistical analysis

All data are expressed as means ± SEM. Statistical analysis was performed using GraphPad Prism 7.0. Sample sizes were according to those used in previous publications from our group and others reporting CSDS. All values use biological replicates and are indicated by group size (n) in figure legends or within bar graphs. Student's *t*-test was used between two-group analysis, and one-way or two-way ANOVA test followed by the Bonferroni's test was used for multi-group analysis. Assessments were considered significant with $P < 0.05$ and non-significant with $P > 0.05$. The detailed statistical information were provided in the Supplemental Information.

3. Results

3.1. TCAs erase m^{6}A epigenetic modification via activating FTO function

To address the effect of antidepressants on m^{6}A modification, in the first section, we incubated N2a neuronal cell line with IMI and AMT for 48 h. By immunofluorescence, we found that both IMI and AMT strongly reduced m^{6}A level in N2a cells (Fig. 1A). By dot blotting, we found that at a therapeutic dosage, intraperitoneal injection (i.p.) of IMI (20 mg/kg, dissolved in saline) and AMT (10 mg/kg, dissolved in saline) for 14 days significantly decreased the global m^{6}A levels in the VTA (Fig. 1B), but did not reduce m^{6}A levels in other brain regions, such as Hip and mPFC (Figs. S1C and D). To elucidate whether IMI also demethylate m^{6}A RNA in the VTA of stressed subjects, CSDS, a social defeat stress-induced depressive model, was used. In the CSDS model, 14 days of IMI was administered indistinctly to susceptible mice that subjected to CSDS, and the global m^{6}A levels in the VTA were also decreased compared with that in the vehicle group (Fig. 1C). We tested the possible mechanisms underlay the effect of TCAs. We incubated N2a neuronal cell line with

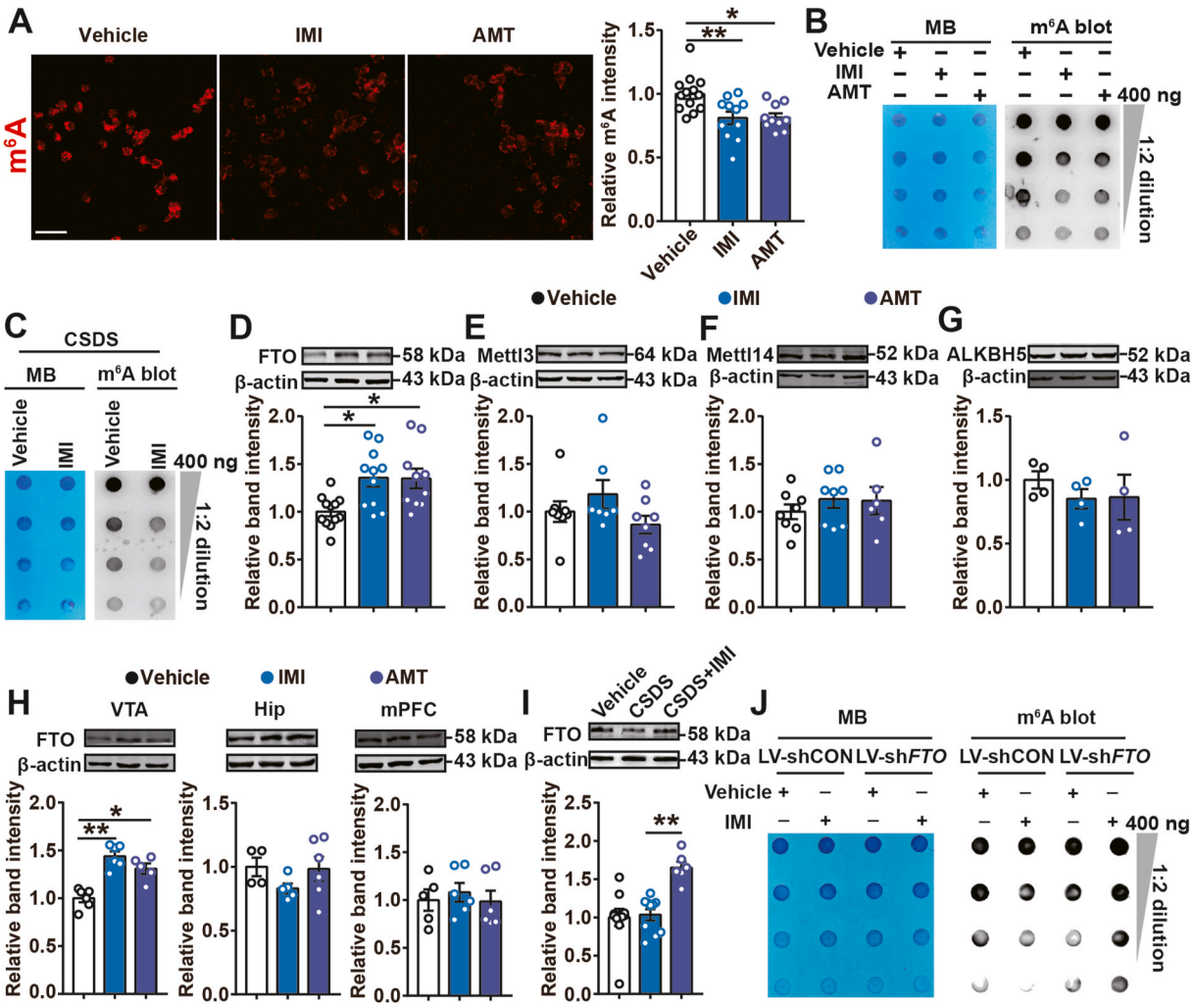

Fig. 1. TCAs erase m^{6}A epigenetic modification via activating FTO function. (A) Immunofluorescence imaging and quantitative analysis of m^{6}A abundance in N2a cells treated with IMI (10 μM), AMT (10 μM) or vehicle for 48 h. Scale bar: 50 μm (n = 10–13 from 4 independent biological replicates, one-way ANOVA, Bonferroni's test). **(B)** Dot blot shows significant decrease in m^{6}A levels in VTA of mice following 14 days treatment with IMI (20 mg/kg, i.p.) or AMT (10 mg/kg, i.p.). **(C)** 14 days of IMI injection indistinctly to susceptible mice subjected to CSDS and m^{6}A levels in VTA was detected by dot blot. **(D–G)** IMI and AMT incubation increased FTO expression in the N2a cells (n = 10–12, one-way ANOVA, Bonferroni's test), but not affected the expression of Mettl3, Mettl14 and ALKBH5 (n = 4–8, one-way ANOVA, Bonferroni's test). **(H)** IMI or AMT significantly increase FTO protein in the VTA (n = 5–6 mice/group, one-way ANOVA, Bonferroni's test), but not in Hip (n = 4–6 mice/group, one-way ANOVA, Bonferroni's test) or mPFC (n = 5–6 mice/group, one-way ANOVA, Bonferroni's test). **(I)** IMI was administered indistinctly for 14 days to susceptible mice that subjected to CSDS, and FTO levels in the VTA were analyzed by western blots (n = 6–10 mice/group, one-way ANOVA, Bonferroni's test). **(J)** Genetically knockdown of FTO in the VTA abolished the effect of IMI on m^{6}A RNA methylation. Data are presented as mean ± SEM. *P < 0.05, **P < 0.01. ANOVA, analysis of variance; N2a, neuroblastoma 2A; IMI, imipramine; AMT, amitriptyline; m^{6}A, N6-methyladenosine; FTO, fat mass and obesity-associated protein; VTA, ventral tegmental area; Hip, hippocampus; mPFC, medial prefrontal cortex; LV, lentivirus; MB, methylene blue; CON, control; CSDS, chronic social defeat stress.

various antidepressants, including IMI, AMT, mirtazapine and fluoxetine, and qPCR analysis indicated that only IMI and AMT increased the mRNA level of FTO (Fig. S1A). Western blotting analysis revealed that IMI and AMT (Fig. 1D) increased, but fluoxetine reduced the FTO expression (Fig. S1B) in the N2a cells. Both IMI and AMT did not affect the expression of Mettl3, Mettl14 and ALKBH5 (Fig. 1E, F, G), highlighting the role of FTO in the epigenetic function of TCAs. Both IMI and AMT are TCAs, and the common tricyclic structure appears to give similar mechanism properties resembling IMI and AMT.

Then, we detected FTO levels in response to antidepressants in different tissues, including the VTA, Hip, mPFC, NAc and liver of mice. Both IMI and AMT increased FTO protein levels in the VTA but not in the Hip, mPFC, NAc, and liver (Fig. 1H, Figs. S2A and B). In the susceptible mice, after IMI treatment for 14 days, FTO also increased significantly in the VTA (Fig. 1I). Genetic disruption of FTO in the VTA by LV-sh*FTO* (Figs. S3A and B) reduced the global m^{6}A levels (Fig. S3C) and largely abolished the reducing effect of IMI on m^{6}A epigenetic modification (Fig. 1J), suggesting a critical role of FTO in the epigenetic function of TCAs.

3.2. *TCAs act by erasing m^{6}A modification via an FTO-dependent manner*

We proceeded to investigate whether m^{6}A erasing effects and FTO mediates the antidepressant effects of TCAs. We pharmacologically mimicked the effect of m^{6}A RNA demethylation using cycloleucine, an inhibitor of RNA methylation. Cycloleucine erased m^{6}A (Fig. S1E) by reducing the cellular levels of S-adenosyl-l-methionine (SAM), the major methyl group donator for DNA and RNA methylation, via competitively inhibiting methionine adenosyltransferase (Jani et al., 2009; Lombardini et al., 1970) that catalyzes the production of SAM from methionine and ATP.

Immobility time in FST and TST of control animals are widely used in

antidepressants screening. Microinjection of cycloleucine in the VTA decreased the immobility time of TST and FST (Fig. 2A), indicating that erasing m^{6}A in the VTA produces antidepressant-like behaviors. Sweet-tasting solutions are a well characterized natural reward and most classic antidepressants did not affect natural reward in control animals, but only reversed stress-induced reduction in sucrose preference, which was considered to be a core anhedonia symptom of depression. After 10 consecutive days of social defeat, the susceptible mice were micro-injected with cycloleucine or vehicle into the VTA, and it was shown that cycloleucine reversed CSDS-induced deficits in sucrose preference and social interactions (Fig. 2B).

Next, we explored the functions of FTO in the effect of antidepressants. Intraperitoneal infusion of rhein (120 mg/kg, dissolved in 0.1% DMSO), an FTO inhibitor, 30 min before administration of IMI and AMT dissipated the antidepressant action of both IMI and AMT in mice (Fig. 2C). Intra-VTA infusion with rhein abolished the effect of IMI on immobility time of TST and FST in mice (Fig. 2D). Furthermore, genetically knockdown of FTO in the VTA abolished the effect of IMI on

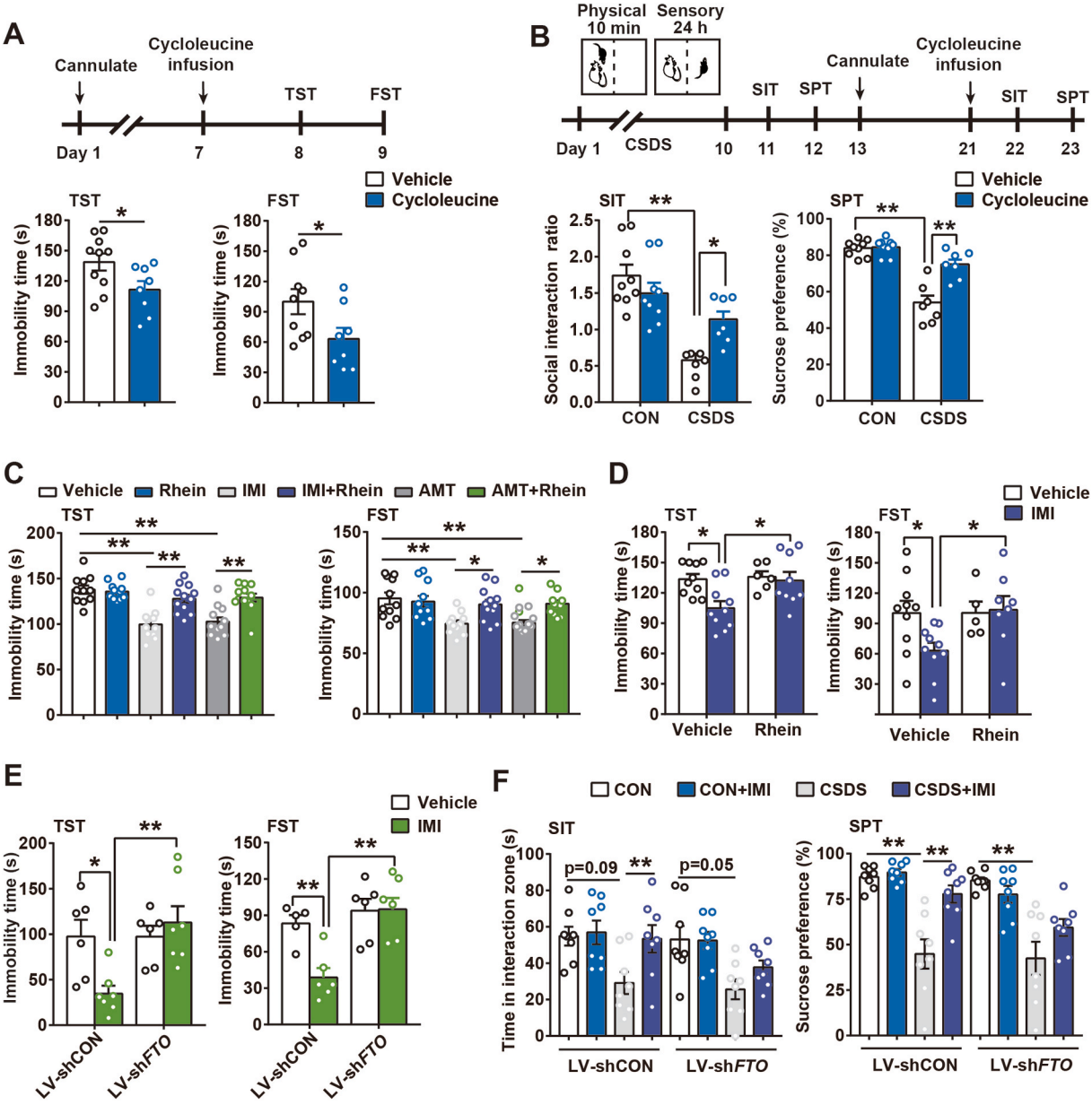

Fig. 2. TCAs act by erasing m^{6}A modification via an FTO-dependent manner. (A, top) Schematic timeline of cycloleucine injection and behavioral tests. Bottom, reducing m^{6}A RNA methylation in the VTA by microinjection of cycloleucine (40 μg/μL/side) decreased the immobility time of TST and FST in mice (n = 8–10 mice/group, Student's *t*-test). **(B, top)** Schematic timeline of CSDS, cycloleucine treatment and behavior tests. Animals were subjected to SIT and SPT before the cannulation to identify the susceptible group, and only the mice with both interaction ratio <1.0 in SIT and sucrose preference <75% in SPT were considered to be susceptible and given vehicle or cycloleucine. Bottom**,** cycloleucine increases social interaction ratio and sucrose preference in susceptible mice (n = 7–9 mice/group, two-way ANOVA, Bonferroni's test). **(C)** Intraperitoneal delivery of rhein (120 mg/kg) blocks the effect of IMI and AMT on immobility time of FST and TST (n = 11–12 mice/group, one-way ANOVA, Bonferroni's test). **(D)** Local bilateral infusion with rhein (1 μg/μL, 1μL/side) eliminated the antidepressant effect of IMI and AMT (n = 5–10 mice/group, two-way ANOVA, Bonferroni's test). **(E)** Genetically knockdown of FTO in the VTA abolished the effect of IMI on immobility time of TST and FST in mice (n = 5–7 mice/group, two-way ANOVA, Bonferroni's test). **(F)** IMI reverses the decrease in social interaction and sucrose preference of stressed mice, while FTO knockdown blocked the therapeutic effect of IMI (n = 8 mice/group, one-way ANOVA, Bonferroni's test). Data are presented as mean ± SEM. *P < 0.05, **P < 0.01. FST, forced swim test; TST, tail suspension test; SPT, sucrose preference test; SIT, social interaction test.

immobility time of TST and FST (Fig. 2E). After viral microinjection of GFP-tagging LV-sh*FTO* or GFP-tagging LV-shCON into the VTA of mice, the mice were subjected to 10 consecutive days of social defeat stress, and the depressed subjects were treated with IMI or a vehicle for two additional weeks. We observed that IMI only reversed the decrease in social interaction and sucrose preference in the mice injected with LV-shCON in the VTA. In contrast, FTO genetic knockdown blocked the therapeutic effect of IMI (Fig. 2F). Thus, FTO in the VTA may play a crucial role in the pharmacology of TCAs.

3.3. FTO in the VTA exerts antidepressant-like action and mediates stress resilience

We sought to determine whether FTO emerges as an endogenous mechanism to mediate stress resilience. First, the effects of AAV-mediated FTO overexpression within the VTA on behavioral despair were measured by the immobility time in two behavioral tests, the TST and FST. Mice were microinjected AAV-FTO or AAV-GFP into the VTA (Fig. 3A). Four weeks later, a marked elevation in the FTO protein level was observed by Western blot (Fig. 3A), and the global m^{6}A levels in the VTA significantly decreased in the FTO-overexpressing mice (Fig. S4A). FTO overexpression in the VTA significantly reduced the immobility time in the TST and FST models (Fig. 3B) and alleviated the anxious behaviors in mice, evaluated by the OFT (Fig. S4B) and EPM (Fig. 3B). Anorexia is a common symptom in depressed individuals, and we found that FTO overexpression in the VTA promoted 2 h and 24 h food intake in control mice with no change in body weight (Figs. S4C and D).

To gain further insight into the role of FTO in the stress resilience, we measured FTO expression in the VTA, Hip and mPFC of mice after social defeat stress. In consistent with the results from susceptible animals in Fig. 1I, CSDS did not alter FTO expression in susceptible group. Interestingly, after CSDS, resilient mice expressed an even higher level of FTO in the VTA than susceptible mice and control mice (Fig. 3C and D), but not in the Hip and mPFC (Fig. 3E and F, Figs. S5A and B). These findings suggest that inducible expression of FTO in the VTA may contribute to stress resilience. After viral microinjection of LV-sh*FTO* or LV-shCON into the VTA, the mice were subjected to a SSDS (three social defeat sessions: 5 min of physical defeat followed by 15 min with no physical defeat). We found that mice injected with LV-sh*FTO* spent less time in the interaction zone and displayed a decreased sucrose preference over that of the LV-shCON mice (Fig. 3G), indicating that FTO may represent an endogenous resilience mechanism.

Then, we evaluated the effect of FTO on the CSDS mice. After 10 consecutive days of social defeat, the susceptible mice were microinjected with AAV-FTO or AAV-GFP into the VTA. FTO overexpression in the VTA significantly increased the time spent with the social target in the interaction zone, ameliorating the social avoidant behavior in stressed individuals (Fig. 3H). Similarly, FTO overexpression also reversed the CSDS-induced decrease in sucrose preference, a behavioral symptom that reflects anhedonia (Fig. 3H). Thus, FTO in the VTA may serve as a target that mediates antidepressant activity.

3.4. Overexpression of FTO oppositely regulates the stress-coupled modifications of transcripts in the VTA

A recent report indicated that stress induced the accumulation of m^{6}A RNA in various brain areas, including the Hip, mPFC and NAc (Engel et al., 2018), but little is known about the VTA. We performed a dot blot analysis and revealed a significant increase in the m^{6}A levels in the VTA of CSDS mice, but not in the Hip or mPFC (Fig. 4A). We hypothesized that the role of VTA m^{6}A may underlie stress susceptibility. To test this idea, we utilized betaine, an activator of m^{6}A RNA methylation, and sought to determine its effect on mice subjected to SSDS. Betaine facilitates m^{6}A formation (Fig. S1F) by increasing the cellular levels of SAM, the major methyl group donator for DNA and RNA methylation, via serving as a substrate for the transmethylation of homocysteine (Lever and Slow, 2010; Narayan and Rottman, 1992). Analogously, we found that mice microinjected with betaine displayed a decreased sucrose preference (Fig. 4B) after SSDS and spent less time in the interaction zone (Fig. 4B).

The m^{6}A modification can alter mRNA expression via multiple mechanisms (Bartosovic et al., 2017; Berulava et al., 2013; Yue et al., 2015). We performed RNA-seq using RNA derived from the VTA of control and susceptible mice to test transcriptional signatures under social stress (Fig. 4C). Using fold-change as a measurement, 235 putative mRNAs were remarkably changed at least 2.0-fold in the mouse transcriptome (Table S1). We hypothesized that the stress-altered transcriptional signature can be oppositely regulated by FTO via its epigenetic role. We observed the transcriptional signature using RNAs derived from the VTA of mice overexpressing AAV-FTO or AAV-GFP, and RNA-seq results revealed that 2032 putative mRNAs were remarkably changed at least 2.0-fold in the mouse transcriptome (Fig. 4C, Table S2). Combining these two RNA-seq results, we found 163 genes in the VTA that were regulated by both FTO and social stress (Fig. S6A, Table S3). We found 23 genes (e.g., *Phf19*, *Pyroxd2*, *etc.* Fig. 4D, Fig. S6B), which were downregulated by social defeat stress but upregulated by FTO overexpression, and 19 genes (e.g., *Cldn2*, *Ndnf*, *etc.* Fig. 4E, Fig. S6C), which were up-regulated in susceptible mice but down-regulated by FTO overexpression. Gene Ontology (GO) analysis (Fig. 4D and E) showed that these different expression genes were highly enriched in pathways related to biological processes, and cellular components. Taken together, these results indicate that FTO may reverse the stress-coupled gene expression network, which may be central to its antidepressant activity.

We selected some candidate overlapping genes (e.g., *Cdh1*, *Rgs14*, *Cox6a2*, *Ucn*, *Cartpt*, *Htr1d* and *Marco*) that most significantly changed in the RNA-seq results of depressed mice as stress-sensitive genes (Fig. S6D) for further verification. Consistent with the RNA-seq data, qPCR analysis (Fig. 4F) found that *Cartpt* (associated with addiction, depression, obesity and insulin resistance), *Htr1d* (associated with type 2 diabetes, depression, schizophrenia, and anorexia) and *Ucn* (associated with anorexia, anxiety, depression, and alcohol drinking) mRNA levels were significantly increased in the VTA of stressed mice, and that *Cdh1* (associated with nerve injury and memory), *Cox6a2* (associated with obesity and insulin resistance), and *Rgs14* (associated with fear memory) mRNA levels were markedly decreased. No significant changes in *Marco* mRNAs were observed (Fig. 4F). Overexpression of FTO oppositely regulates the stress-coupled transcripts changes in the VTA of stressed mice (Fig. 4G).

3.5. Erasing m^{6}A-dependent methylation of mRNAs encoding stress-sensitive peptides may underlie the antidepressant activity of FTO and TCAs

Since FTO expression was promoted by TCAs, we next explored whether IMI could alter the expression of overlapping candidate genes. After CSDS, susceptible mice were treated by IMI or vehicle for 14 days, and the overlapping candidate genes was tested. After 14 days of IMI treatment, decreased levels of *Cartpt* and *Ucn* and increased levels of *Cad1, Cox6a2* and *Rgs14* in the VTA were observed (Fig. 5A), consistent with the results of FTO overexpression (Fig. 4G), suggesting that both FTO and antidepressants inversely regulated the social stress-related transcriptional profile in the VTA. Interestingly, after 14 days, only two candidate genes encoding stress-sensitive neuropeptides, *Cartpt* and *Ucn,* remained significantly altered in the vehicle group, which was reversed to normal only by IMI. Genetic inhibition of FTO in the VTA via LV-sh*FTO* eliminated the effect of IMI on *Ucn* and *Cartpt* in the stressed mice (Fig. 5B). Then, we explored whether *Ucn* and *Cartpt* were associated with stress resilience. Local bilateral infusion of recombinant UCN (1 μg/μL, 1 μL per side) and CART (0.5 μg/μL, 1 μL per side) protein into the VTA reduced the time spent in the interaction zone and resulted in decreased sucrose preference (Fig. 5C) after SSDS. These lines highlight

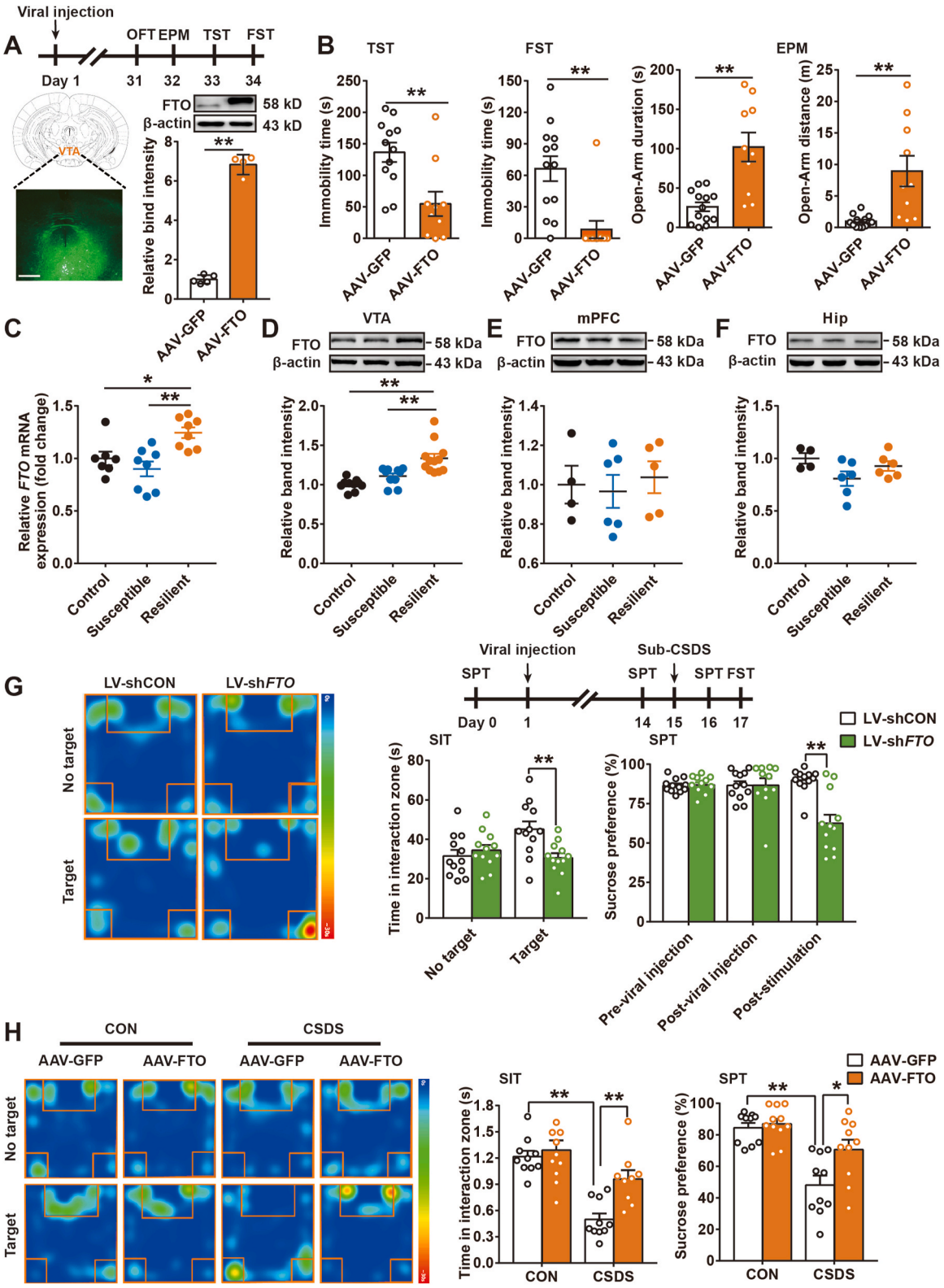

Fig. 3. FTO in the VTA confers antidepressant activity and stress resilience. (A, top) Schematic timeline of adeno-associated virus injection and behavioral tests. Bottom, representative photomicrograph of injection sites (left) in the VTA. Scale bars, 100 μm. Western blot analysis of FTO protein level in VTA (right) four weeks after injection with AAV-GFP/AAV-FTO (n = 4–5 mice/group, Student's *t*-test). **(B)** AAV-FTO viral expression in the VTA decreased the immobility time of TST and FST, increased open arm time and distance of EPM (n = 10–13 mice/group, Student's *t*-test). **(C)** FTO mRNA expression in the VTA of control, susceptible and resilient mice (n = 7–8 mice/group, one-way ANOVA, Bonferroni's test). **(D–F)** Western blots analysis of FTO protein levels in the VTA, Hip and mPFC of control, susceptible and resilient mice (n = 4–12 mice/group, one-way ANOVA, Bonferroni's test). (**G**) LV-sh*FTO* viral expression in the VTA decreased social interaction time with target and sucrose preference following SSDS (n = 11–12 mice/group, two-way ANOVA, Bonferroni's test). **(H)** AAV-FTO viral expression in the VTA increased sucrose preference and social interaction time with target in the stressed mice (n = 9–11 mice/group, two-way ANOVA, Bonferroni's test). Data are presented as mean ± SEM. *P < 0.05, **P < 0.01. AAV, adeno-associated virus; EPM, elevated plus maze; GFP, green fluorescent protein; SSDS, subthreshold social defeat stress.

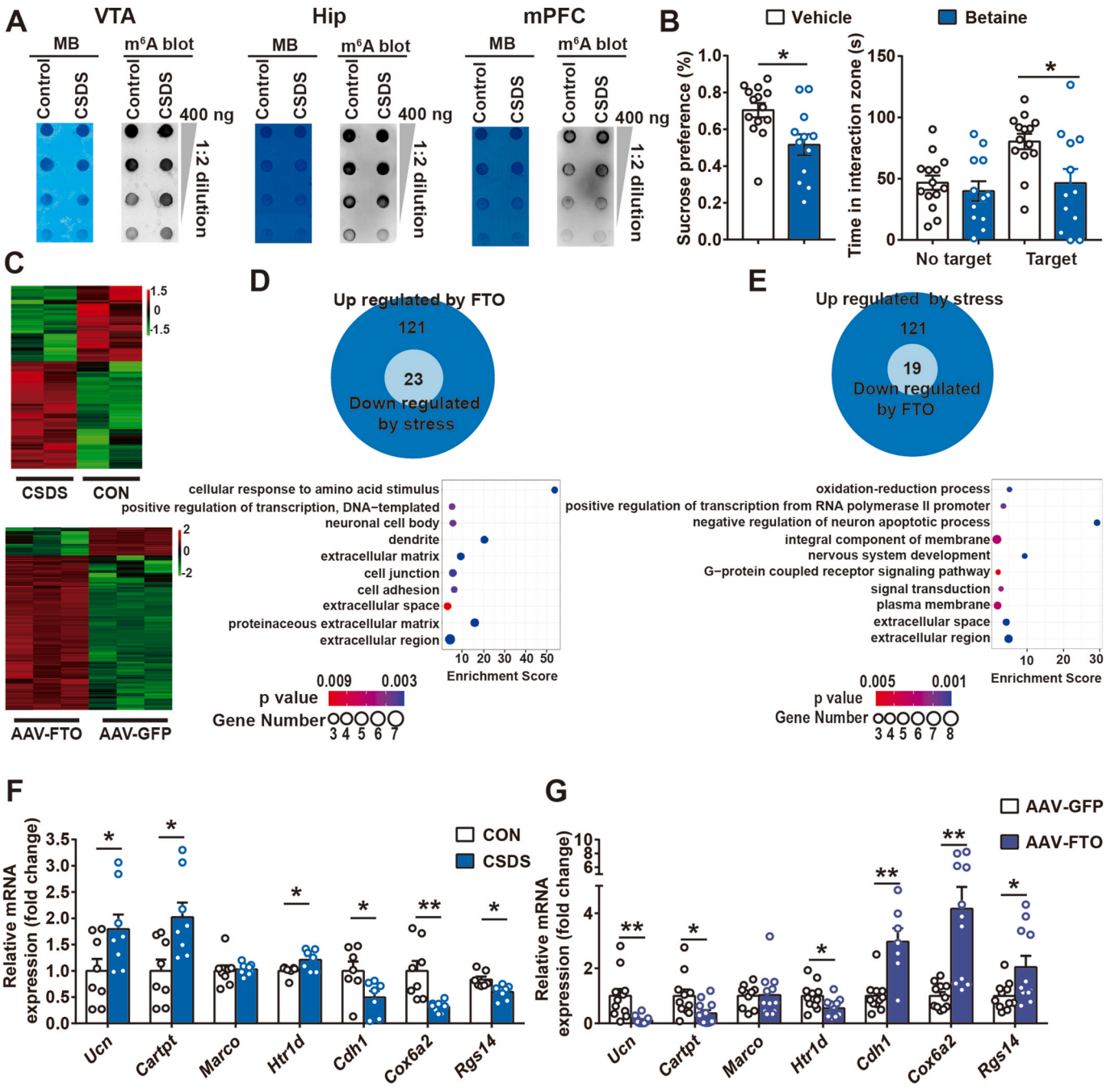

Fig. 4. FTO overexpression in the VTA reverses the altered transcriptional signature under social defeat stress. (A) Dot blot detects m^{6}A levels in the VTA, Hip and mPFC of susceptible mice. (**B**) Locally bilateral infusion of betaine (20 μg/μL, 1 μL per side), an activator of m^{6}A RNA methylation, decreases sucrose preference (n = 12–14 mice/group, Student's *t*-test) and social interaction time (n = 12–14 mice/group, one-way ANOVA, Bonferroni's test) of mice underwent subthreshold social defeat stress. (**C, top**) Heatmap of CSDS-induced expression changes in the VTA as compared to control mice. Bottom, heatmap of FTO overexpression-regulated expression changes in the VTA compared to mice injected with AAV-GFP. **(D, top)** Venn diagram depicts the overlap of different expression genes (DEGs) between downregulated in depressed mice and upregulated by FTO overexpression. Bottom, bubble chart displaying the top ten gene ontology categories with downregulated in depressed mice and upregulated by FTO overexpression ($P < 0.05$ or fold-change ≥ 2.0). (**E, top**) The Venn diagram showing common and specific DEGs upregulated in the susceptible mice and downregulated by FTO overexpression. Bottom, the top ten significantly enriched categories associated with upregulated in depressed mice and downregulated by FTO overexpression. **(F)** qPCR analysis of mRNAs in the VTA of stressed mice. (n = 7–8 mice/group, Student's *t*-test). **(G)** qPCR analysis of mRNAs in the VTA of susceptible mice injected with AAV-FTO. (n = 7–12 mice/group, Student's *t*-test). Data are presented as mean ± SEM. *P < 0.05, **P < 0.01. *Ucn, urocotin*; *Cartpt cocaine- and amphetamine-regulated transcript prepropeptide*; *Cdh1, cadherin 1*; *Rgs14, regulator of G protein signaling 14*; *Htr1d, 5-hydroxytryptamine receptor 1D*; *Cox6a2, cytochrome c oxidase subunit 6A2*; *Marco, macrophage receptor with collagenous structure*.

a critical role of stress-sensitive neuropeptides such as CART and UCN in the antidepressant activity of TCAs. Considering the important role of FTO in RNA demethylation, the m^{6}A status was detected via MeRIP-qPCR (Fig. 5D). SRAMP, a sequence-based m^{6}A modification site predictor (Zhou et al., 2016), revealed five m^{6}A modification sites in the mRNA sequence of *Ucn* and three m^{6}A modification sites in the mRNA sequence of *Cartpt* (Fig. 5E). Specific primers against m^{6}A sites located in the CDS region were designed to amplify products. Increased m^{6}A levels were found in fragmented RNA from the VTA of stressed mice (Fig. 5F). Overexpression of FTO alleviated m^{6}A methylation of *Ucn* and *Cartpt* in

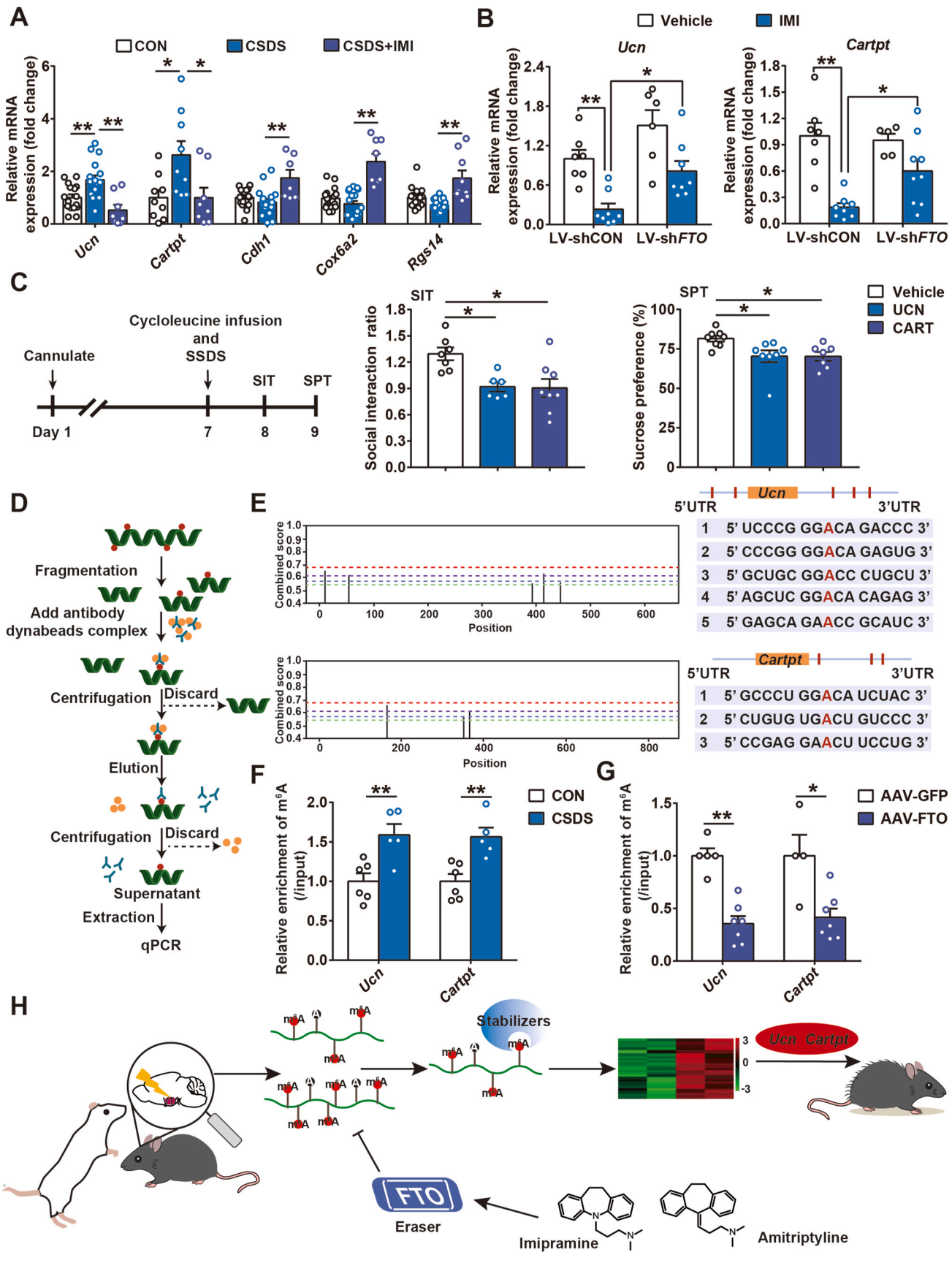

(caption on next page)

Fig. 5. Erasing m^{6}A-dependent methylation of mRNAs that encoding stress-sensitive peptides underlies the antidepressant activity of FTO and TCAs. **(A)** qPCR analysis of overlapping candidate genes in the VTA of control and CSDS mice after chronic IMI treatment (n = 7–19 mice/group, one-way ANOVA, Bonferroni's test). **(B)** Genetically down-regulation of FTO in the VTA of stressed mice eliminate the changes in *Ucn* and *Cartpt* mRNA levels induce by IMI (n = 5–9 mice/group, two-way ANOVA, Bonferroni's test). **(C)** Schematic timeline (left) and behavioral consequences of UCN and CART recombinant protein in the SIT (middle), SPT (right) after subthreshold social defeat stress (n = 6–8 mice/group, one-way ANOVA, Bonferroni's test). **(D)** A Flowchart for MeRIP-qPCR. **(E)** Predictive m^{6}A sites of *Ucn* and *Cartpt* mRNA in SRAMP. **(F)** The m^{6}A status of *Ucn* and *Cartpt* increased in the stressed mice (n = 5–6 mice/group, Student's *t*-test). **(G)** MeRIP-qPCR showed a decrease in m^{6}A modification of *Ucn* and *Cartpt* in the stressed mice with FTO overexpression in the VTA (n = 4–7 mice/group, Student's *t*-test). **(H)** Schematic diagrams of tricyclics produce an antidepressant activity via initiating an FTO-dependent regulation of stress-related m^{6}A modification. Data are presented as mean ± SEM. *P < 0.05, **P < 0.01. MeRIP, methylated RNA immunoprecipitation.

the VTA of stressed mice (Fig. 5G). In summary, IMI may act as an antidepressant by activating FTO-dependent m^{6}A demethylation to regulate the transcription of stress-sensitive genes such as *Cartpt* and *Ucn* (Fig. 5H).

4. Discussion

FTO is traditionally thought to work in epigenetic regulation as a vital nucleic acid demethylase. Here, we found a novel and unexpectedly beneficial function of FTO under social stress. Another surprising finding is that a previously unrecognized link between m^{6}A modification and antidepressant pharmacology has been revealed. Tricyclics may produce antidepressant activity via initiating an FTO-dependent regulation of stress-related m^{6}A modification, followed by a reversal of a stress-coupled transcriptional signature in the VTA (Fig. 5H). Thus, our findings shed new light on conceptually novel antidepressants that function through the potentiation of FTO function.

The evidence that fostered the general TCA pharmacology mainly originated from the monoamine hypothesis. However, the monoamine hypothesis has been questioned because the antidepressant effect of TCAs is not clearly associated with the monoaminergic effect. The investigation of TCA pharmacology profoundly inspired and supported the findings of MDD mechanisms, such as the dysfunction in neurogenesis and the activation of acid sphingomyelinase (Gulbins et al., 2013; Kornhuber et al., 2014; Santarelli et al., 2003; Warner-Schmidt and Duman, 2006). Here, we report that the FTO-mediated demethylation of m^{6}A emerged as a novel target for TCAs. TCAs increased the expression of FTO both in vitro and *in vivo*, and a disruption of FTO by pharmacological approaches or VTA-specific genetic approaches led to a significant abolishment of the antidepressant effect of TCAs. The increase of FTO expression occurred after TCA treatment for two weeks, which was in consistent with the antidepressant effect delay. The promoting effect on FTO expression seems to be closely related to the structure and general pharmacological properties of TCAs. Interestingly, weight gain is a common adverse effect of TCAs (Berken et al., 1984; Salvi et al., 2018; Serretti and Porcelli, 2018). FTO is an obesity- and diabetes-related protein owing to the linkage between its genetic polymorphism and body mass index (BMI). Previous reports and our results have demonstrated that FTO overexpression leads to increased food intake (Church et al., 2010), which may result from the alterations of dopamine D2-like receptor function to influence reward-related food intake (Hess et al., 2013) and FTO-associated increase in body mass may result primarily from increased food intake. More recent studies have indicated that FTO may facilitate weight gain by shifting the endocrine balance from the satiety hormone leptin toward the hunger-promoting hormone ghrelin (Benedict et al., 2014; Karra et al., 2013). Our study has revealed that TCAs increased FTO expression in the VTA, a central brain region for the control of food-related processes, and raised a previously unrecognized link between the weight effect and antidepressant pharmacology. Thus, an activation of FTO function may represent a previously unrecognized link between the weight effect and antidepressant pharmacology. Given the predicted association of FTO with antipsychotic-induced weight gain (Shing et al., 2014) and our findings about FTO-mediated antidepressant effect, FTO may be critical to determine whether antidepressant exerts therapeutic effect or adverse effect. Blockade of FTO downstream genes that participate in weight gain but not in stress resistance possibly alleviate the drug-induced weight gain, which may confer a new strategy for much safer treatment for depression in the future. Our findings raise novel insights into the TCAs pharmacology.

The present study highlights a novel neurobiological function of FTO, the RNA demethylase that has attracted much attention in recent years. An increasing number of studies have demonstrated that FTO plays vital roles in many biological processes, ranging from brain development (Ma et al., 2018) and cell metabolism (Merkestein et al., 2015; Speakman, 2015) to tumor procession (Li et al., 2017b). We reported that FTO-dependent m^{6}A demethylation determines the vulnerability to social stress. These results, along with recent observations that FTO controls neurogenesis (Li et al., 2017a) and regulates memory formation (Spychala and Ruther, 2019), raised the possibility that FTO may serve as a target for developing novel rapid antidepressants. In our study, virus-mediated overexpression was used to investigate the action of FTO, and we found that overexpression of FTO in the VTA significantly reduced the immobility time in the TST and FST, alleviated the anxious behaviors in mice (Fig. 3B) and social avoidant behavior in stressed individuals (Fig. 3H), and promoted food intake (Figs. S4C and D). Virus-mediated overexpression of FTO increased FTO level to 6.83 ± 0.25 fold in the VTA, and FTO expression was increased to 1.33 ± 0.06 fold in the VTA in resilient mice. Meanwhile, IMI treatment increased FTO expression to 1.44 ± 0.05 fold in the VTA. Although stress resilience and TCAs could not completely mimic the effect of virus-mediated overexpression, they both produced some similar behavioral effects, such as improved social interactions or reduced behavioral despair.

It should be noted that FTO may affect various brain functions, thus, identification of FTO downstream genes to mediate antidepressant effects may bring novel targets for development of antidepressants. We observed that an overexpression of FTO altered the expression of more than 2195 genes. GO analysis implied that numerous genes regulate cell proliferation, differentiation, or metabolism, among which the expression of 398 RNAs were under tight regulation by social stress. Thus, FTO may work via oppositely regulation of the stress-coupled transcriptional signature in the VTA. In Fig. 4F, qPCR analysis found that *Cartpt*, *Htr1d*, *Ucn*, *Cdh1*, *Cox6a2*, and *Rgs14* mRNA levels were markedly altered by CSDS. However, in Fig. 5A, only *Cartpt* and *Ucn* displayed significant alterations in the vehicle group. The discrepancies between Figs. 4F and 5G may be resulted from that, animals in Fig. 4F were sacrificed after CSDS, but animals in Fig. 5A were sacrificed after a two-week treatment of vehicle or IMI following CSDS, which may buffer some CSDS-induced alterations of gene expression. Additionally, injections of vehicle or IMI for two weeks induced some levels of other stress. Thus, only genes that were more strongly dysregulated by social defeat stress, such as *Cartpt* and *Ucn*, were detected in the experimental conditions of Fig. 5G. The peptide encoded by *Cartpt* has been revealed as a candidate biomarker for MDD because of its effects on emotion and distribution covering brain areas involved in the mood regulation, via interactions with neurotransmitter receptors, such as dopamine receptors, glutamate receptors and γ-aminobutyric acid receptors (Ahmadian-Moghadam et al., 2018; Upadhya et al., 2012; Wiehager et al., 2009), which may bridge the interaction between the stress-related events and the neurobehavioral response (Chaki et al., 2003; Walker et al., 2021). Urocortin peptides, including Ucn1, Ucn 2 and Ucn3, acts on the corticotropin-releasing factor receptors to elicit stress responses (Ma

et al., 2020), modulate social behavior (Deussing and Chen, 2018) and controll stress-related disorders (Romero-Leguizamon and Kohlmeier, 2020; Wang et al., 2007), including anxiety and depression. As a member of the corticotropin-releasing factor (CRF) family, Ucn1 acts as a CRF1 receptor agonist to elicit anxiety- and depression-like behaviors via activating HPA axis (Kormos and Gaszner, 2013; Tsatsanis et al., 2007). However, until now, the precise mechanisms underlying stress responses regulation by *Ucn* and *Cartpt* remain unclear. FTO overexpression inhibited CSDS-triggered transcription of *Cartpt* and *Ucn*, which may underlie the pathophysiology of depression. TCAs reduced CSDS-triggered transcription of *Cartpt* and *Ucn*, which may be involved in their pharmacology.

Epigenetic changes that cause modifications of a gene's functional state without changing its coding sequence have emerged as possible pivotal regulatory mechanisms in the pathogenesis of psychiatric diseases (Hess et al., 2013; Zheng et al., 2013), and psychoactive drugs may act by impacting epigenetic machinery, such as modulating stress-induced DNA methylation and histone deacetylation (Bohnsack et al., 2019; Shafik et al., 2021). Many studies have revealed that changes in DNA methylation, histone modifications and noncoding RNAs contribute to stress-induced depression-like behavior (Lin and Gregory, 2014; Yue et al., 2015; Zhao et al., 2014). As a novel epigenetic machinery, m^6A has been shown to regulate gene expression by modulating pre-mRNA splicing, mRNA stability, RNA structure, and pre-miRNA processing (Lopez et al., 2014; Sales et al., 2011; Tadic et al., 2014). Here, we found that stress-coupled m^6A modifications of transcripts in the VTA altered the expression of *Cartpt* and *Ucn*. Reversal of stress-induced m^6A modification by FTO replenished the alterations in the transcript network. Our study successfully showed *in vivo* evidence of m^6A writing/erasing in CNS diseases.

It should be noted that several problems needed to be resolved in the next study. In the present study, the mechanisms underlying stress resilience-coupled FTO expression in the VTA remains unknown. Considering that dopamine neurons in the VTA are sensitive to stress, which mediates stress susceptibility and resilience, and a recent study (Hu et al., 2020) has reported that glucocorticoid receptor-dependent FTO transactivation induces lipid accumulation in hepatocytes, we hypothesized that a glucocorticoid-regulated FTO expression in the VTA may contribute to stress resilience. Further investigation is required. Although FTO may reverse the social stress-coupled modifications of candidate gene transcripts in the VTA, much less is known about the precise mechanism. For instance, FTO down-regulated the m^6A methylation of *Carpt* and *Ucn*, but decreased their expression. m^6A modifications altered gene expression via multiple mechanisms. A m^6A-IP-seq should be performed to confirm these alterations and clarify the mechanism in the future. We speculated that this was probably due to the multiple functions of m^6A modification in RNA splicing, nuclear export, and protein translation. Although stress-related peptides including *Ucn* and *Cartpt* were important downstream genes of FTO-mediated antidepressant effects, RNA-seq data and qPCR analysis revealed other stress-related genes that regulated by FTO, such as *Htr1d* and *Rgs14*. *Htr1d* control serotonin release, and its alterations may contribute to the increased synaptic serotonin levels underlying depression and antidepressant response (Honda et al., 2004; Whale et al., 2001). *Rgs14* is a multifunctional signaling protein that regulates postsynaptic plasticity in neurons to affect memory, emotion, and stimulus-induced behaviors (Harbin et al., 2021; Lee et al., 2010). These altered genes may also be involved in the pathogenesis of depression.

In conclusion, we discovered that targeting stress-coupled m^6A mRNA epigenetic modifications to reverse transcriptional signature may work as a novel antidepressant strategy. Furthermore, our results suggest that FTO and its downstream genes are molecular targets for the development of novel antidepressants.

Declaration of competing interest

The authors declare no competing financial interests.

CRediT authorship contribution statement

Peng-Fei Wu: Conceptualization, Methodology, Data curation, Formal analysis, Writing – original draft, Funding acquisition. **Qian-Qian Han:** Methodology, Investigation, Writing – original draft. **Fu-Feng Chen:** Investigation, Methodology, Validation. **Tian-Tian Shen:** Investigation, Methodology, Validation. **Yi-Heng Li:** Investigation, Methodology, Validation. **Yu Cao:** Investigation, Methodology, Validation. **Jian-Guo Chen:** Writing – review & editing, Project administration, Supervision, Funding acquisition. **Fang Wang:** Writing – review & editing, Project administration, Supervision, Funding acquisition.

Acknowledgements

This work was supported by grants from the Foundation for Innovative Research Groups of NSFC (No. 81721005 to J.G.C. and F. W.), National Natural Science Foundation of China (No. 81773712 to P.F.W., No. 81971279 to F.W., No. 81973310 to J.G.C.), National Key R&D Program of China (No. 2020YFA0803900) and PCSIRT (No. IRT13016) to J.G.C., the Program for Integrated Innovative Team for Major Human Diseases Program of Tongji Medical College, HUST, to F. W.

Appendix A. Supplementary data

Supplementary data to this article can be found online at https://doi.org/10.1016/j.ynstr.2021.100390.

References

Ahmadian-Moghadam, H., Sadat-Shirazi, M.S., Zarrindast, M.R., 2018. Cocaine- and amphetamine-regulated transcript (CART): a multifaceted neuropeptide. Peptides 110, 56–77. https://doi.org/10.1016/j.peptides.2018.10.008.

Bartosovic, M., Molares, H.C., Gregorova, P., Hrossova, D., Kudla, G., Vanacova, S., 2017. N6-methyladenosine demethylase FTO targets pre-mRNAs and regulates alternative splicing and 3'-end processing. Nucleic Acids Res. 45, 11356–11370. https://doi.org/10.1093/nar/gkx778.

Benedict, C., Axelsson, T., Soderberg, S., Larsson, A., Ingelsson, E., Lind, L., et al., 2014. Fat mass and obesity-associated gene (FTO) is linked to higher plasma levels of the hunger hormone ghrelin and lower serum levels of the satiety hormone leptin in older adults. Diabetes 63, 3955–3959. https://doi.org/10.2337/db14-0470.

Berken, G.H., Weinstein, D.O., Stern, W.C., 1984. Weight gain. A side-effect of tricyclic antidepressants. J. Affect. Disord. 7, 133–138. https://doi.org/10.1016/0165-0327(84)90031-4.

Berulava, T., Ziehe, M., Klein-Hitpass, L., Mladenov, E., Thomale, J., Ruther, U., et al., 2013. FTO levels affect RNA modification and the transcriptome. Eur. J. Hum. Genet. 21, 317–323. https://doi.org/10.1038/ejhg.2012.168.

Bohnsack, J.P., Teppen, T., Kyzar, E.J., Dzitoyeva, S., Pandey, S.C., 2019. The lncRNA BDNF-AS is an epigenetic regulator in the human amygdala in early onset alcohol use disorders. Transl. Psychiatry 9, 34. https://doi.org/10.1038/s41398-019-0367-z.

Chaki, S., Kawashima, N., Suzuki, Y., Shimazaki, T., Okuyama, S., 2003. Cocaine- and amphetamine-regulated transcript peptide produces anxiety-like behavior in rodents. Eur. J. Pharmacol. 464, 49–54. https://doi.org/10.1016/s0014-2999(03)01368-2.

Chen, B., Ye, F., Yu, L., Jia, G., Huang, X., Zhang, X., et al., 2012. Development of cell-active N6-methyladenosine RNA demethylase FTO inhibitor. J. Am. Chem. Soc. 134, 17963–17971. https://doi.org/10.1021/ja3064149.

Chen, J., Zhang, Y.C., Huang, C., Shen, H., Sun, B., Cheng, X., et al., 2019. m(6)A regulates neurogenesis and neuronal development by modulating histone methyltransferase Ezh2. Dev. Reprod. Biol. 17, 154–168. https://doi.org/10.1016/j.gpb.2018.12.007.

Church, C., Moir, L., McMurray, F., Girard, C., Banks, G.T., Teboul, L., et al., 2010. Overexpression of Fto leads to increased food intake and results in obesity. Nat. Genet. 42, 1086–1092. https://doi.org/10.1038/ng.713.

Deussing, J.M., Chen, A., 2018. The corticotropin-releasing factor family: physiology of the stress response. Physiol. Rev. 98, 2225–2286. https://doi.org/10.1152/physrev.00042.2017.

Dominissini, D., Moshitch-Moshkovitz, S., Salmon-Divon, M., Amariglio, N., Rechavi, G., 2013. Transcriptome-wide mapping of N(6)-methyladenosine by m(6)A-seq based on immunocapturing and massively parallel sequencing. Nat. Protoc. 8, 176–189. https://doi.org/10.1038/nprot.2012.148.

Edens, B.M., Vissers, C., Su, J., Arumugam, S., Xu, Z., Shi, H., et al., 2019. FMRP modulates neural differentiation through m(6)a-dependent mRNA nuclear export. Cell Rep. 28, 845–854. https://doi.org/10.1016/j.celrep.2019.06.072 e845.

Engel, M., Eggert, C., Kaplick, P.M., Eder, M., Roh, S., Tietze, L., et al., 2018. The role of m(6)A/m-RNA methylation in stress response regulation. Neuron 99, 389–403. https://doi.org/10.1016/j.neuron.2018.07.009 e389.

Frayling, T.M., Timpson, N.J., Weedon, M.N., Zeggini, E., Freathy, R.M., Lindgren, C.M., et al., 2007. A common variant in the FTO gene is associated with body mass index and predisposes to childhood and adult obesity. Science 316, 889–894. https://doi.org/10.1126/science.1141634.

Friedman, A.K., Juarez, B., Ku, S.M., Zhang, H.X., Calizo, R.C., Walsh, J.J., et al., 2016. KCNQ channel openers reverse depressive symptoms via an active resilience mechanism. Nat. Commun. 7 https://doi.org/10.1038/ncomms11671.

Gao, H., Cheng, X., Chen, J., Ji, C., Guo, H., Qu, W., et al., 2020. Fto-modulated lipid niche regulates adult neurogenesis through modulating adenosine metabolism. Hum. Mol. Genet. 29, 2775–2787. https://doi.org/10.1093/hmg/ddaa171.

Gulbins, A., Schumacher, F., Becker, K.A., Wilker, B., Soddemann, M., Boldrin, F., et al., 2018. Antidepressants act by inducing autophagy controlled by sphingomyelin-ceramide. Mol. Psychiatr. 23, 2324–2346. https://doi.org/10.1038/s41380-018-0090-9.

Gulbins, E., Palmada, M., Reichel, M., Luth, A., Bohmer, C., Amato, D., et al., 2013. Acid sphingomyelinase-ceramide system mediates effects of antidepressant drugs. Nat. Med. 19, 934–938. https://doi.org/10.1038/nm.3214.

Harbin, N.H., Bramlett, S.N., Montanez-Miranda, C., Terzioglu, G., Hepler, J.R., 2021. RGS14 regulation of post-synaptic signaling and spine plasticity in brain. Int. J. Mol. Sci. 22 https://doi.org/10.3390/ijms22136823.

He, J.G., Zhou, H.Y., Xue, S.G., Lu, J.J., Xu, J.F., Zhou, B., et al., 2021. Transcription factor TWIST1 integrates dendritic remodeling and chronic stress to promote depressive-like behaviors. Biol. Psychiatr. 89, 615–626. https://doi.org/10.1016/j.biopsych.2020.09.003.

Hess, M.E., Hess, S., Meyer, K.D., Verhagen, L.A., Koch, L., Bronneke, H.S., et al., 2013. The fat mass and obesity associated gene (Fto) regulates activity of the dopaminergic midbrain circuitry. Nat. Neurosci. 16, 1042–1048. https://doi.org/10.1038/nn.3449.

Honda, M., Imaida, K., Tanabe, M., Ono, H., 2004. Endogenously released 5-hydroxytryptamine depresses the spinal monosynaptic reflex via 5-HT1D receptors. Eur. J. Pharmacol. 503, 55–61. https://doi.org/10.1016/j.ejphar.2004.09.045.

Hu, Y., Feng, Y., Zhang, L.C., Jia, Y.M., Cai, D.M., Qian, S.B., et al., 2020. GR-mediated FTO transactivation induces lipid accumulation in hepatocytes via demethylation of m(6)A on lipogenic mRNAs. RNA Biol. 17, 930–942. https://doi.org/10.1080/15476286.2020.1736868.

Huang, R., Zhang, Y., Bai, Y., Han, B., Ju, M., Chen, B., et al., 2020. N(6)-Methyladenosine modification of fatty acid amide hydrolase messenger RNA in circular RNA STAG1-regulated astrocyte dysfunction and depressive-like behaviors. Biol. Psychiatr. 88, 392–404. https://doi.org/10.1016/j.biopsych.2020.02.018.

Jani, T.S., Gobejishvili, L., Hote, P.T., Barve, A.S., Joshi-Barve, S., Kharebava, G., et al., 2009. Inhibition of methionine adenosyltransferase II induces FasL expression, Fas-DISC formation and caspase-8-dependent apoptotic death in T leukemic cells. Cell Res. 19, 358–369. https://doi.org/10.1038/cr.2008.314.

Jia, G., Fu, Y., Zhao, X., Dai, Q., Zheng, G., Yang, Y., et al., 2011. N6-methyladenosine in nuclear RNA is a major substrate of the obesity-associated FTO. Nat. Chem. Biol. 7, 885–887. https://doi.org/10.1038/nchembio.687.

Karra, E., O'Daly, O.G., Choudhury, A.I., Yousseif, A., Millership, S., Neary, M.T., et al., 2013. A link between FTO, ghrelin, and impaired brain food-cue responsivity. J. Clin. Invest. 123, 3539–3551. https://doi.org/10.1172/Jci44403.

Klinsey, S.G., Bailey, M.T., Sheridan, J.F., Padgett, D.A., Avitsur, R., 2007. Repeated social defeat causes increased anxiety-like behavior and alters splenocyte function in C57BL/6 and CD-1 mice. Brain Behav. Immun. 21, 458–466. https://doi.org/10.1016/j.bbi.2006.11.001.

Kormos, V., Gaszner, B., 2013. Role of neuropeptides in anxiety, stress, and depression: from animals to humans. Neuropeptides 47, 401–419. https://doi.org/10.1016/j.npep.2013.10.014.

Kornhuber, J., Muller, C.P., Becker, K.A., Reichel, M., Gulbins, E., 2014. The ceramide system as a novel antidepressant target. Trends Pharmacol. Sci. 35, 293–304. https://doi.org/10.1016/j.tips.2014.04.003.

Lee, S.E., Simons, S.B., Heldt, S.A., Zhao, M.L., Schroeder, J.P., Vellano, C.P., et al., 2010. RGS14 is a natural suppressor of both synaptic plasticity in CA2 neurons and hippocampal-based learning and memory. Proc. Natl. Acad. Sci. U. S. A 107, 16994–16998. https://doi.org/10.1073/pnas.1005362107.

Lever, M., Slow, S., 2010. The clinical significance of betaine, an osmolyte with a key role in methyl group metabolism. Clin. Biochem. 43, 732–744. https://doi.org/10.1016/j.clinbiochem.2010.03.009.

Li, L., Zang, L., Zhang, F., Chen, J., Shen, H., Shu, L., et al., 2017a. Fat mass and obesity-associated (FTO) protein regulates adult neurogenesis. Hum. Mol. Genet. 26, 2398–2411. https://doi.org/10.1093/hmg/ddx128.

Li, M.X., Zheng, H.L., Luo, Y., He, J.G., Wang, W., Han, J., et al., 2018. Gene deficiency and pharmacological inhibition of caspase-1 confers resilience to chronic social defeat stress via regulating the stability of surface AMPARs. Mol. Psychiatr. 23, 556–568. https://doi.org/10.1038/mp.2017.76.

Li, Z., Weng, H., Su, R., Weng, X., Zuo, Z., Li, C., et al., 2017b. FTO plays an oncogenic role in acute myeloid leukemia as a N(6)-methyladenosine RNA demethylase. Canc. Cell 31, 127–141. https://doi.org/10.1016/j.ccell.2016.11.017.

Lin, S., Gregory, R.I., 2014. Methyltransferases modulate RNA stability in embryonic stem cells. Nat. Cell Biol. 16, 129–131. https://doi.org/10.1038/ncb2914.

Liu, J., Yue, Y., Han, D., Wang, X., Fu, Y., Zhang, L., et al., 2014. A METTL3-METTL14 complex mediates mammalian nuclear RNA N6-adenosine methylation. Nat. Chem. Biol. 10, 93–95. https://doi.org/10.1038/nchembio.1432.

Lombardini, J.B., Coulter, A.W., Talalay, P., 1970. Analogues of methionine as substrates and inhibitors of the methionine adenosyltransferase reaction. Deductions concerning the conformation of methionine. Mol. Pharmacol. 6, 481–499.

Lopez, J.P., Lim, R., Cruceanu, C., Crapper, L., Fasano, C., Labonte, B., et al., 2014. miR-1202 is a primate-specific and brain-enriched microRNA involved in major depression and antidepressant treatment. Nat. Med. 20, 764–768. https://doi.org/10.1038/nm.3582.

Ma, C., Chang, M., Lv, H., Zhang, Z.W., Zhang, W., He, X., et al., 2018. RNA m(6)A methylation participates in regulation of postnatal development of the mouse cerebellum. Genome Biol. 19, 68. https://doi.org/10.1186/s13059-018-1435-z.

Ma, S., Shen, Q., Zhao, L.H., Mao, C., Zhou, X.E., Shen, D.D., et al., 2020. Molecular basis for hormone recognition and activation of corticotropin-releasing factor receptors. Mol. Cell. 77, 669–680. https://doi.org/10.1016/j.molcel.2020.01.013 e664.

Merkestein, M., Laber, S., McMurray, F., Andrew, D., Sachse, G., Sanderson, J., et al., 2015. FTO influences adipogenesis by regulating mitotic clonal expansion. Nat. Commun. 6, 6792. https://doi.org/10.1038/ncomms7792.

Merkurjev, D., Hong, W.T., Iida, K., Oomoto, I., Goldie, B.J., Yamaguti, H., et al., 2018. Synaptic N(6)-methyladenosine (m(6)A) epitranscriptome reveals functional partitioning of localized transcripts. Nat. Neurosci. 21, 1004–1014. https://doi.org/10.1038/s41593-018-0173-6.

Narayan, P., Rottman, F.M., 1992. Methylation of mRNA. Adv. Enzymol. Relat. Area Mol. Biol. 65, 255–285. https://doi.org/10.1002/9780470123119.ch7.

Peng, S., Xiao, W., Ju, D., Sun, B., Hou, N., Liu, Q., et al., 2019. Identification of entacapone as a chemical inhibitor of FTO mediating metabolic regulation through FOXO1. Sci. Transl. Med. 11 https://doi.org/10.1126/scitranslmed.aau7116.

Ping, X.L., Sun, B.F., Wang, L., Xiao, W., Yang, X., Wang, W.J., et al., 2014. Mammalian WTAP is a regulatory subunit of the RNA N6-methyladenosine methyltransferase. Cell Res. 24, 177–189. https://doi.org/10.1038/cr.2014.3.

Romero-Leguizamon, C.R., Kohlmeier, K.A., 2020. Stress-related endogenous neuropeptides induce neuronal excitation in the Laterodorsal Tegmentum. Eur. Neuropsychopharmacol 38, 86–97. https://doi.org/10.1016/j.euroneuro.2020.07.008.

Sales, A.J., Biojone, C., Terceti, M.S., Guimaraes, F.S., Gomes, M.V., Joca, S.R., 2011. Antidepressant-like effect induced by systemic and intra-hippocampal administration of DNA methylation inhibitors. Br. J. Pharmacol. 164, 1711–1721. https://doi.org/10.1111/j.1476-5381.2011.01489.x.

Salvi, V., Mencacci, C., Barone-Adesi, F., 2018. Antidepressant induced weight gain associated with anti-histaminergic activity. BMJ 362, k3222. https://doi.org/10.1136/bmj.k3222.

Santarelli, L., Saxe, M., Gross, C., Surget, A., Battaglia, F., Dulawa, S., et al., 2003. Requirement of hippocampal neurogenesis for the behavioral effects of antidepressants. Science 301, 805–809. https://doi.org/10.1126/science.1083328.

Serretti, A., Porcelli, S., 2018. Antidepressant induced weight gain. BMJ 361, k2151. https://doi.org/10.1136/bmj.k2151.

Shafik, A.M., Zhang, F., Guo, Z., Dai, Q., Pajdzik, K., Li, Y., et al., 2021. N6-methyladenosine dynamics in neurodevelopment and aging, and its potential role in Alzheimer's disease. Genome Biol. 22, 17. https://doi.org/10.1186/s13059-020-02249-z.

Shing, E.C., Tiwari, A.K., Brandl, E.J., Zai, C.C., Lieberman, J.A., Meltzer, H.Y., et al., 2014. Fat mass- and obesity-associated (FTO) gene and antipsychotic-induced weight gain: an association study. Neuropsychobiology 69, 59–63. https://doi.org/10.1159/000356231.

Speakman, J.R., 2015. The 'fat mass and obesity related' (FTO) gene: mechanisms of impact on obesity and energy balance. Curr. Obes. Rep. 4, 73–91. https://doi.org/10.1007/s13679-015-0143-1.

Spychala, A., Ruther, U., 2019. FTO affects hippocampal function by regulation of BDNF processing. PloS One 14, e0211937. https://doi.org/10.1371/journal.pone.0211937.

Su, R., Dong, L., Li, C., Nachtergaele, S., Wunderlich, M., Qing, Y., et al., 2018. R-2HG exhibits anti-tumor activity by targeting FTO/m(6)A/MYC/CEBPA signaling. Cell 172, 90–105. https://doi.org/10.1016/j.cell.2017.11.031 e123.

Tadic, A., Muller-Engling, L., Schlicht, K.F., Kotsiari, A., Dreimuller, N., Kleimann, A., et al., 2014. Methylation of the promoter of brain-derived neurotrophic factor exon IV and antidepressant response in major depression. Mol. Psychiatr. 19, 281–283. https://doi.org/10.1038/mp.2013.58.

Tsatsanis, C., Dermitzaki, E., Venihaki, M., Chatzaki, E., Minas, V., Gravanis, A., et al., 2007. The corticotropin-releasing factor (CRF) family of peptides as local modulators of adrenal function. Cell. Mol. Life Sci. 64, 1638–1655. https://doi.org/10.1007/s00018-007-6555-7.

Upadhya, M.A., Nakhate, K.T., Kokare, D.M., Singh, U., Singru, P.S., Subhedar, N.K., 2012. CART peptide in the nucleus accumbens shell acts downstream to dopamine and mediates the reward and reinforcement actions of morphine. Neuropharmacology 62, 1823–1833. https://doi.org/10.1016/j.neuropharm.2011.12.004.

Walker, L.C., Hand, L.J., Letherby, B., Huckstep, K.L., Campbell, E.J., Lawrence, A.J., 2021. Cocaine and amphetamine regulated transcript (CART) signalling in the central nucleus of the amygdala modulates stress-induced alcohol seeking. Neuropsychopharmacology 46, 325–333. https://doi.org/10.1038/s41386-020-00807-4.

Wang, B., You, Z.B., Rice, K.C., Wise, R.A., 2007. Stress-induced relapse to cocaine seeking: roles for the CRF(2) receptor and CRF-binding protein in the ventral tegmental area of the rat. Psychopharmacology (Berlin) 193, 283–294. https://doi.org/10.1007/s00213-007-0782-3.

Wang, X., Feng, J., Xue, Y., Guan, Z., Zhang, D., Liu, Z., et al., 2016. Structural basis of N (6)-adenosine methylation by the METTL3-METTL14 complex. Nature 534, 575–578. https://doi.org/10.1038/nature18298.

Warner-Schmidt, J.L., Duman, R.S., 2006. Hippocampal neurogenesis: opposing effects of stress and antidepressant treatment. Hippocampus 16, 239–249. https://doi.org/10.1002/hipo.20156.

Whale, R., Clifford, E.M., Bhagwagar, Z., Cowen, P.J., 2001. Decreased sensitivity of 5-HT(1D) receptors in melancholic depression. Br. J. Psychiatry 178, 454–457. https://doi.org/10.1192/bjp.178.5.454.

Widagdo, J., Zhao, Q.Y., Kempen, M.J., Tan, M.C., Ratnu, V.S., Wei, W., et al., 2016. Experience-dependent accumulation of N6-methyladenosine in the prefrontal cortex is associated with memory processes in mice. J. Neurosci. 36, 6771–6777. https://doi.org/10.1523/JNEUROSCI.4053-15.2016.

Wiehager, S., Beiderbeck, D.I., Gruber, S.H., El-Khoury, A., Wamsteeker, J., Neumann, I. D., et al., 2009. Increased levels of cocaine and amphetamine regulated transcript in two animal models of depression and anxiety. Neurobiol. Dis. 34, 375–380. https://doi.org/10.1016/j.nbd.2009.02.010.

Wu, R., Li, A., Sun, B., Sun, J.G., Zhang, J., Zhang, T., et al., 2019. A novel m(6)A reader Prrc2a controls oligodendroglial specification and myelination. Cell Res. 29, 23–41. https://doi.org/10.1038/s41422-018-0113-8.

Yohn, C.N., Dieterich, A., Bazer, A.S., Maita, I., Giedraitis, M., Samuels, B.A., 2019. Chronic non-discriminatory social defeat is an effective chronic stress paradigm for both male and female mice. Neuropsychopharmacology 44, 2220–2229. https://doi.org/10.1038/s41386-019-0520-7.

Yue, Y., Liu, J., He, C., 2015. RNA N6-methyladenosine methylation in post-transcriptional gene expression regulation. Genes Dev. 29, 1343–1355. https://doi.org/10.1101/gad.262766.115.

Zhao, X., Yang, Y., Sun, B.F., Shi, Y., Yang, X., Xiao, W., et al., 2014. FTO-dependent demethylation of N6-methyladenosine regulates mRNA splicing and is required for adipogenesis. Cell Res. 24, 1403–1419. https://doi.org/10.1038/cr.2014.151.

Zheng, G., Dahl, J.A., Niu, Y., Fedorcsak, P., Huang, C.M., Li, C.J., et al., 2013. ALKBH5 is a mammalian RNA demethylase that impacts RNA metabolism and mouse fertility. Mol. Cell. 49, 18–29. https://doi.org/10.1016/j.molcel.2012.10.015.

Zhou, Y., Zeng, P., Li, Y.H., Zhang, Z., Cui, Q., 2016. SRAMP: prediction of mammalian N6-methyladenosine (m6A) sites based on sequence-derived features. Nucleic Acids Res. 44, e91. https://doi.org/10.1093/nar/gkw104.